# Technical Report

| | |
|---|---|
| **Program and KPI:** | Sub-program 1.1 KPI 2.7 & Sub-program 1.3 KPI 2.17 |
| **Report Title:** | Report on antenna and probe design for portable microwave system |
| **Prepared by:** | Jayaseelan Marimuthu and Venkata Pamarla<br>Murdoch University |
| **Date published:** | 30 June 2021 |



*This project is supported by funding from the Australian Government Department of Agriculture, Fisheries and Forestry as part of its Rural R&D for Profit programme in partnership with Research & Development Corporations, Commercial Companies, State Departments & Universities.*

## Citation

Marimuthu J., & Pamarla. V (2021). Report on antenna and probe design for portable microwave system. June, 29 pp

## Acknowledgements

This study was undertaken through the Advanced Livestock Measurement Technologies Project (ALMTech) and funded by the Department of Agriculture Rural Research and Development (R&D) for Profit program and Meat and Livestock Australia. Meat and Livestock Australia are thanked for their funding for data acquisition, and for access to commercial herds to compile the calibration datasets.



*This project is supported by funding from the Australian Government Department of Agriculture, Fisheries and Forestry as part of its Rural R&D for Profit programme in partnership with Research & Development Corporations, Commercial Companies, State Departments & Universities.*

# Abstract

Experiment One details the design and computer simulation of three different probe/antenna performance to penetrate fat and muscle. The Vivaldi Patch Antenna (VPA) had the widest radiation pattern, where as the open-ended coaxial probe (OCP) has a directional radiation pattern. The periodic log antenna (PLA) demonstrated a high gain at a low frequency, however at higher frequencies the gain unexpectedly decreased making it unsuitable for deep tissue measurements.

Experiment Two details the commercial comparison of the VPA, OCP and PLA on sheep and beef carcases. Predicting beef carcase P8 fat depth, the PLA demonstrated the greatest precision of prediction with an average RMSEP of 1.29 mm and $R^2$ of 0.83. Predicting lamb carcase C-site and GR fat depth the VPA and PLA had similar prediction performance where the OCP had a lower precision of prediction. In Experiment B the VPA C-site prediction had an average RMSEP of 0.94 mm and $R^2$ of 0.67 where as the OCP had an average RMSEP of 1.04 mm and $R^2$ or 0.56. Experiment B VPA GR site prediction had an average RMSEP of 2.80 mm and $R^2$ of 0.67 vs the OCP average RMSEP of 3.31 mm and $R^2$ of 0.56. Experiment C VPA C-site prediction was similar to Experiment B, with an average RMSEP of 1.02 mm and $R^2$ of 0.66. Experiment C PLA average RMSEP was 1.00 mm and $R^2$ 0.67. However Experiment C VPA GR tissue depth prediction was less than Experiment B with an average RMSEP of 3.57 mm and $R^2$ of 0.55. Experiment C PLA GR site prediction was similar to VPA with an average RMSEP of 3.70 mm and $R^2$ of 0.50.



*This project is supported by funding from the Australian Government Department of Agriculture, Fisheries and Forestry as part of its Rural R&D for Profit programme in partnership with Research & Development Corporations, Commercial Companies, State Departments & Universities.*

# Executive Summary

- To enable signal penetration deep into the tissues, antennas need to be compact and operate at a low frequency of 0.7 GHz – 3GHz.
- VPA has the widest radiation pattern, most suitable for measuring multiple traits from one point on the carcase
- OCP has a smaller directional radiation pattern, suitable for deep single-site tissue measurements
- PLA has a high gain at low frequencies, making it suitable for measurements of small tissue depth such as subcutaneous fat, however as the frequency increases the gain decreases making it unsuitable for deep muscle measurements.
- VPA and PLA had similar performance to predict single-site subcutaneous carcase fatness in beef and lamb. In the commercial setting the OCP did not perform as well as the VPA and PLA for predicting single site fatness.



*This project is supported by funding from the Australian Government Department of Agriculture, Fisheries and Forestry as part of its Rural R&D for Profit programme in partnership with Research & Development Corporations, Commercial Companies, State Departments & Universities.*

# Contents





*This project is supported by funding from the Australian Government Department of Agriculture, Fisheries and Forestry as part of its Rural R&D for Profit programme in partnership with Research & Development Corporations, Commercial Companies, State Departments & Universities.*

*This project is supported by funding from the Australian Government Department of Agriculture, Fisheries and Forestry as part of its Rural R&D for Profit programme in partnership with Research & Development Corporations, Commercial Companies, State Departments & Universities.*

# 1 Milestone description

KPI 2.7.1 Report on the continued improvement of the antennae and probe design for use of the portable microwave system in commercial feedlots.

KPI 2.17.1 Report on the continued improvement of the antenna and probe design for use of the portable microwave system in commercial abattoirs.

# 2 Project objectives

The overall objective of this work is for the continuous research and development on new antenna/probe designs and analysis of tissue layers to integrate it to portable microwave system for the commercial testing at feedlots and abattoirs.

# 3 Experiment One – antenna/probe design & simulation

This experiment evaluates different antenna designs and performance comparisons on tissues (fat and muscle) and its electromagnetic waves interactions at different stepped frequencies in a simulation environment. The antennas were designed and tested in CST™ and Feko (Altair 2021) electromagnetic simulation software's for reflection co-efficient (S11), gain, far-field, and near-field radiation pattern. Different tissue layers were constructed (skin, fat, muscle and bone) for the visualisation of electromagnetic waves interactions on tissue layers and compare antenna penetrations ability to predict the C-Site/GR Tissue/p8 site/rib fat depths on sheep and cattle.

## 3.1 Antenna/probe design and radiation pattern

Three varying designs; a Vivaldi Patch Antenna (VPA), open-ended coaxial probe (OCP) and periodic log antenna (PLA) were designed using CST™ simulation software and tested in a simulation environment.

### 3.1.1 Vivaldi Patch Antenna

The VPA antenna consists of thirteen exponential corrugations on top and bottom of the patches. Fig 1 shows the cross section view of VPA antenna when placed Infront of tissues. The antenna was designed on Rogers R03010 substrate with dielectric permittivity of 10.2 and loss tangent of 0.0022. The antenna was designed to operate in the frequency range of 1 – 6 GHz. Fig 2 shows the simulation of free space reflection coefficient (S11) and response of reflected signal when antenna is placed Infront of tissues. Fig 3 shows the gain of antenna throughout the design frequency range. Fig 4 shows the far field radiation pattern at 2 GHz, 2.5 GHz, 3 GHz, and 3.5 GHz. The main lobe radiation direction for the far-field pattern is 90$^{o}$.



*This project is supported by funding from the Australian Government Department of Agriculture, Fisheries and Forestry as part of its Rural R&D for Profit programme in partnership with Research & Development Corporations, Commercial Companies, State Departments & Universities.*

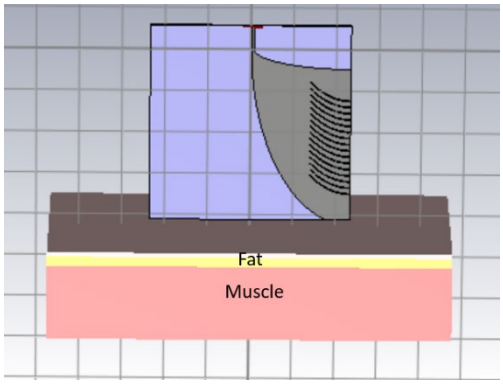


**Figure 1 Cross-section view of VPA antenna on fat and muscle**

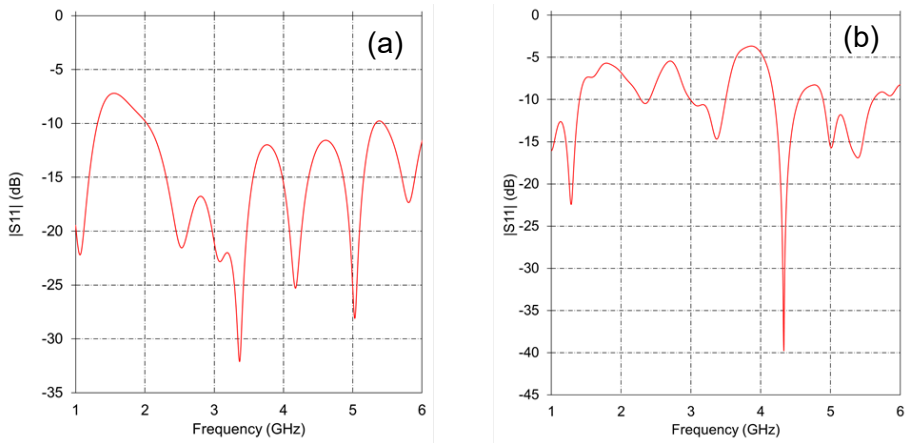


**Figure 2 VPA (a) free space reflection coefficient layers (b) reflection coefficient with tissue layers**

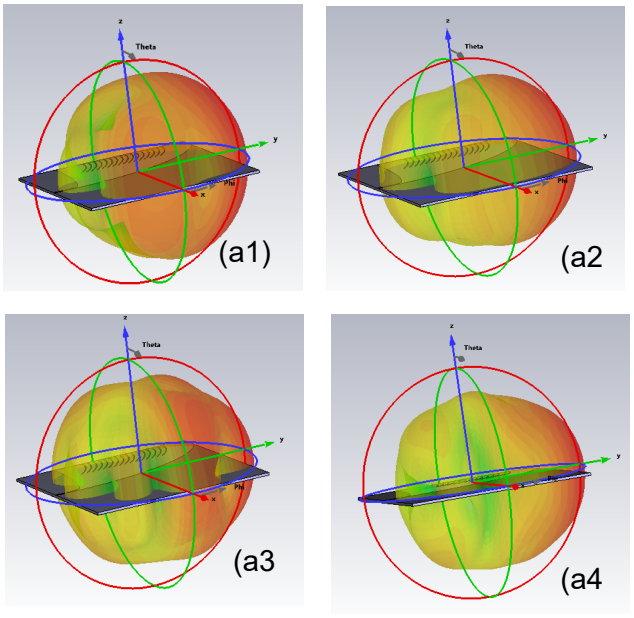


**Figure 3 3D far field radiation pattern of VPA antenna (a1) 2 GHz (a2) 2.5 GHz (a3) 3 GHz (a4) 4 GHz**



*This project is supported by funding from the Australian Government Department of Agriculture, Fisheries and Forestry as part of its Rural R&D for Profit programme in partnership with Research & Development Corporations, Commercial Companies, State Departments & Universities.*

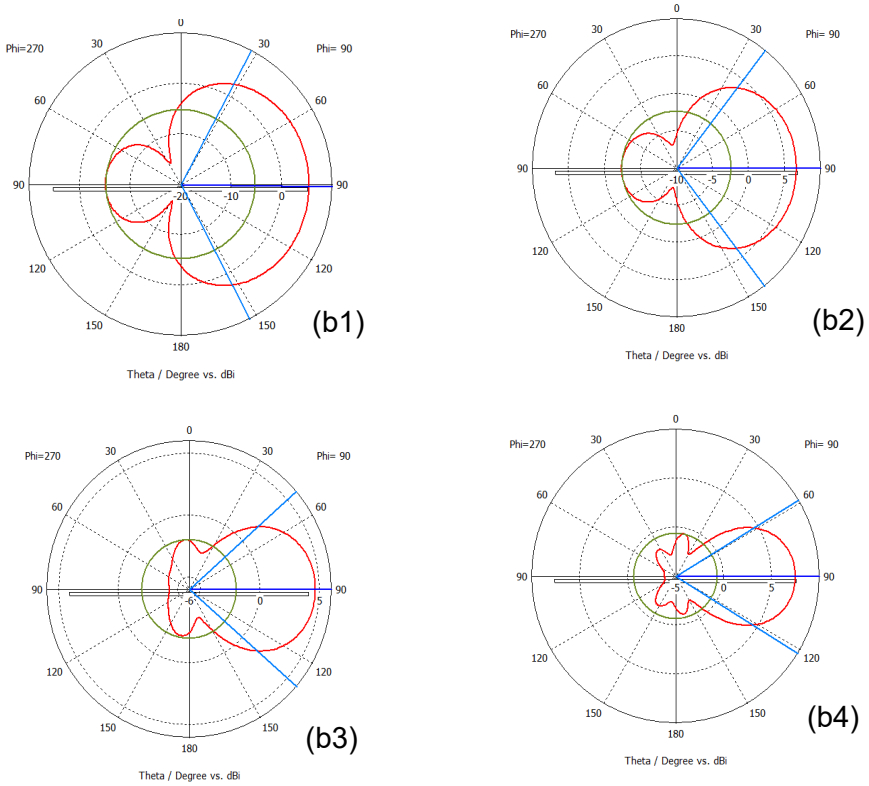


**Figure 4 1D far field polar plot of VPA antenna (b1) 2 GHz (b2) 2.5 GHz (b3) 3 GHz (b4) 4 GHz**



*This project is supported by funding from the Australian Government Department of Agriculture, Fisheries and Forestry as part of its Rural R&D for Profit programme in partnership with Research & Development Corporations, Commercial Companies, State Departments & Universities.*

### 3.1.2 Open-ended coaxial probe

The OCP consists of a truncated section of a transmission lines. The electromagnetic field propagates along the coaxial line and reflection occurs when the electromagnetic field encounters an impedance mismatch between the probe and the tissue sample. The open-ended coaxial probe can also support TE and TM waveguide modes in addition to the TEM mode. The current probe is designed to operate in TEM mode (Pozar, 2011). Fig 5 Shows the cross-section view of open-ended coaxial probe on fat and muscle. Fig 6 shows the free space reflection coefficient along with the response of reflected signal when placed Infront of fat and muscle. OCP probe operation and mechanism are different than VPA and PL antennas. As the electromagnetic waves propagate through the inner conductor and the fields are confined to a smaller and narrow region of the probe and near-field contour plot is the best way to visualise the radiation pattern of the OCP probe than a far-field radiation pattern. Fig 7 shows the near-field radiation pattern of the OCP probe in free space.

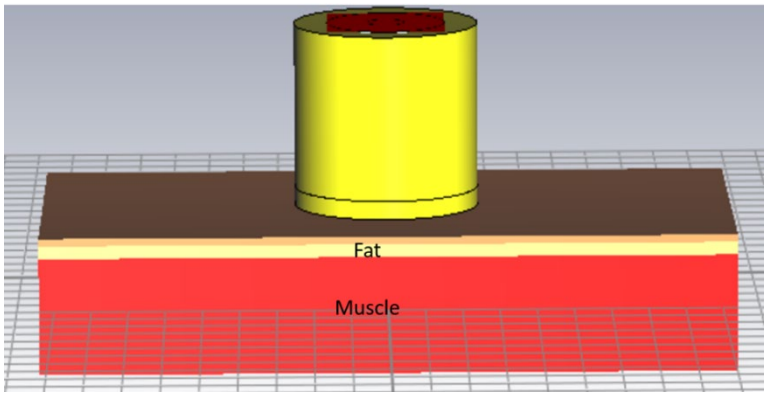


**Figure 5 Cross-section view of open-ended coaxial probe on fat and muscle tissues**

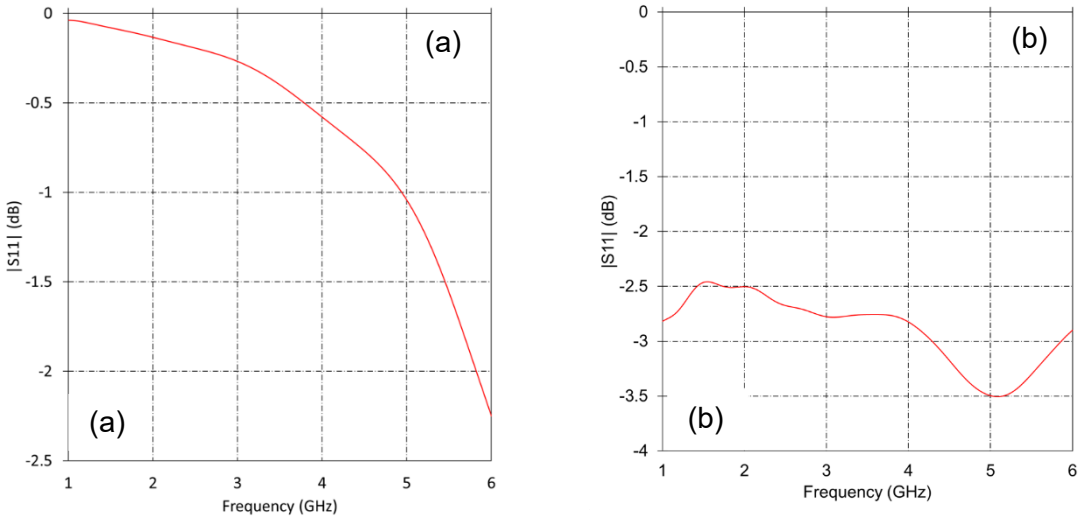


**Figure 6 Open-ended coaxial probe (a) free space reflection coefficient layers (b) reflection coefficient with tissue**



*This project is supported by funding from the Australian Government Department of Agriculture, Fisheries and Forestry as part of its Rural R&D for Profit programme in partnership with Research & Development Corporations, Commercial Companies, State Departments & Universities.*

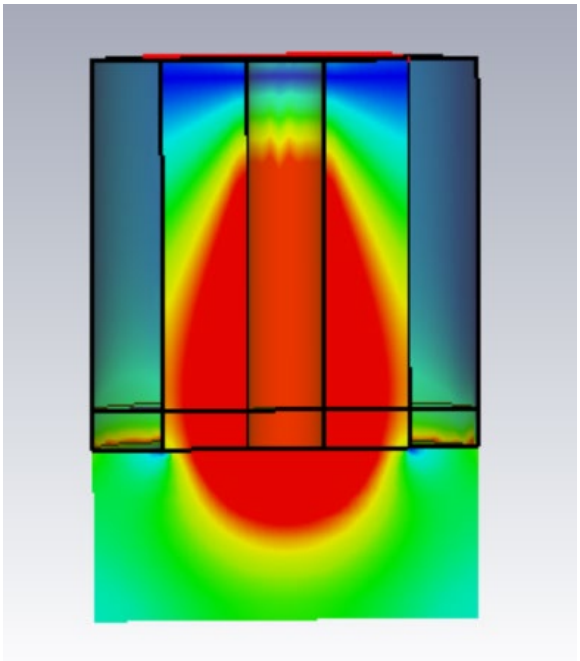

**Figure 7 Near-field contour plot of OCP probe in free space**

### 3.1.3 Periodic-Log antenna

Periodic log/ log-periodic antenna is multielement directional antenna designed to operate over a wide band frequency. The antenna consists of several half-wave dipole driven elements gradually increasing length and consists of metal rods/strip lines adjacent to each other. LPDA antenna looks like yagi antenna and the metal rods/strip lines are connected via centre rod/boom/strip line (Sushko, Piltyay, & Dubrovka, 2020). Fig. 8 shows the cross section view of PLA antenna on fat and muscle tissues. The antenna was designed on Rogers R03010 substrate with dielectric permittivity of 10.2 and loss tangent of 0.0022. The antenna was designed to operate in the frequency range of 1 – 6 GHz. Fig. 9 shows the reflection coefficient (S11) of the PLA antenna along with the reflected signal response when placed Infront of fat and muscle tissues. Fig. 10 shows the 3D far field radiation pattern at 2 GHz, 2.5 GHz, 3 GHz and 3.5 GHz and Fig. 11 shows the 1D far field polar plot at 2 GHz,2.5 GHz, 3GHz and 3.5 GHz. The main lobe radiation direction for the far-field pattern for the PLA is 90$^{o}$, the same as the VPA (Fig.4).



*This project is supported by funding from the Australian Government Department of Agriculture, Fisheries and Forestry as part of its Rural R&D for Profit programme in partnership with Research & Development Corporations, Commercial Companies, State Departments & Universities.*

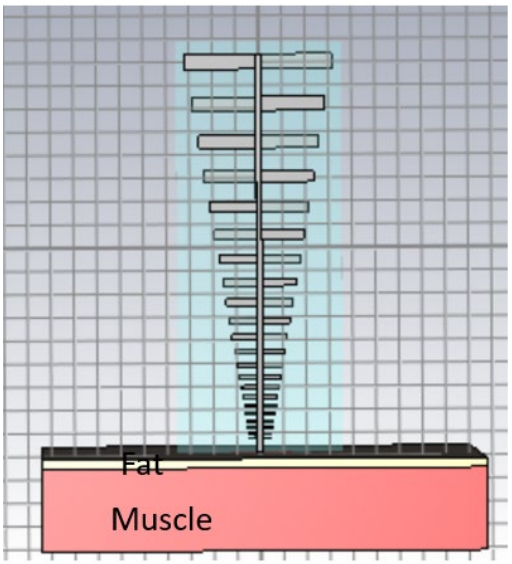


**Figure 8 Cross section view of PLA antenna on fat and muscle**

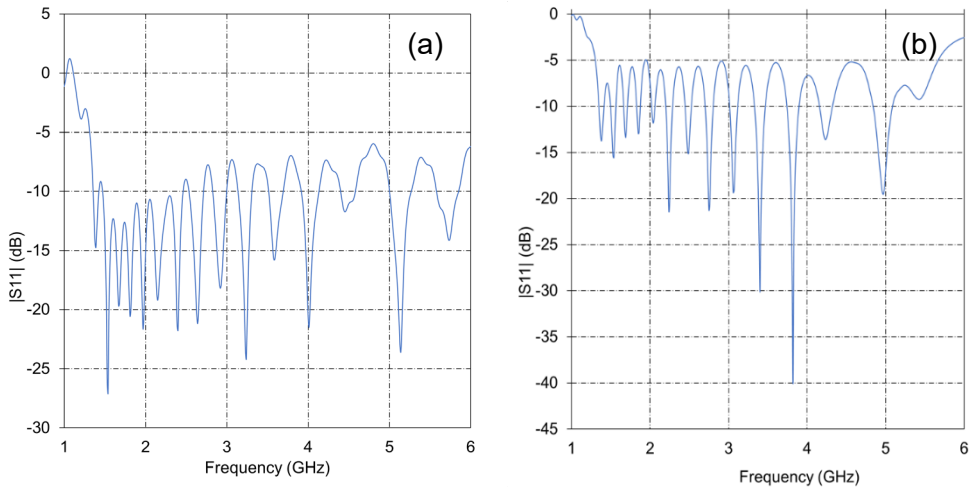


**Figure 9 PLA (a) free space reflection coefficient layers (b) reflection coefficient with tissue**



*This project is supported by funding from the Australian Government Department of Agriculture, Fisheries and Forestry as part of its Rural R&D for Profit programme in partnership with Research & Development Corporations, Commercial Companies, State Departments & Universities.*

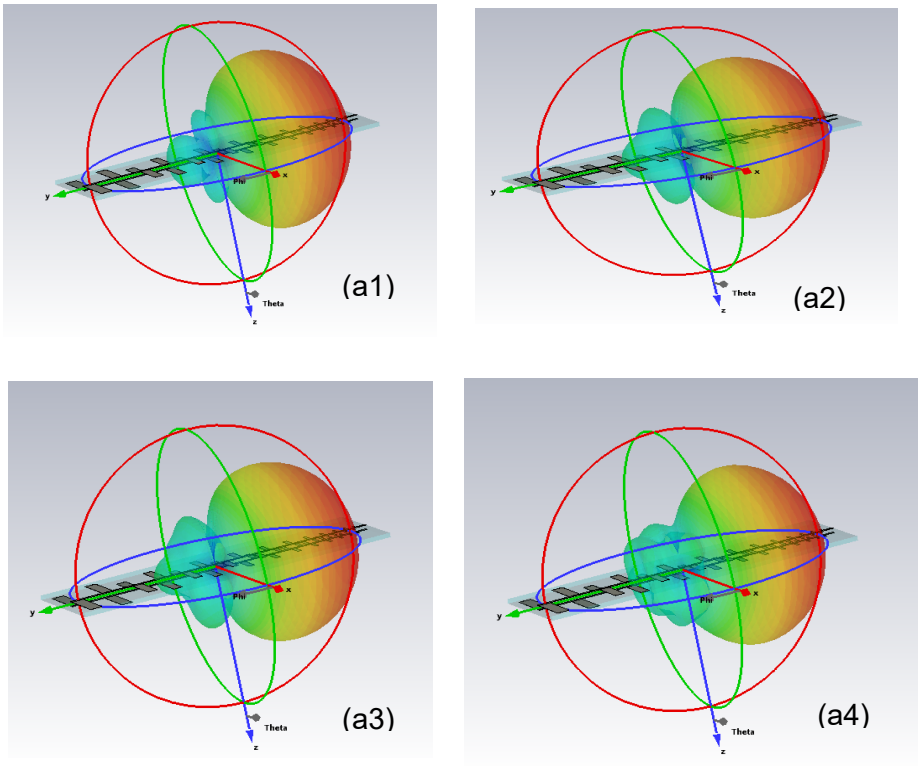


**Figure 10 3D far -field radiation pattern of PLA antenna (a1) 2 GHz (a2) 2.5 GHz (a3) 3 GHz (a4) 4 GHz**

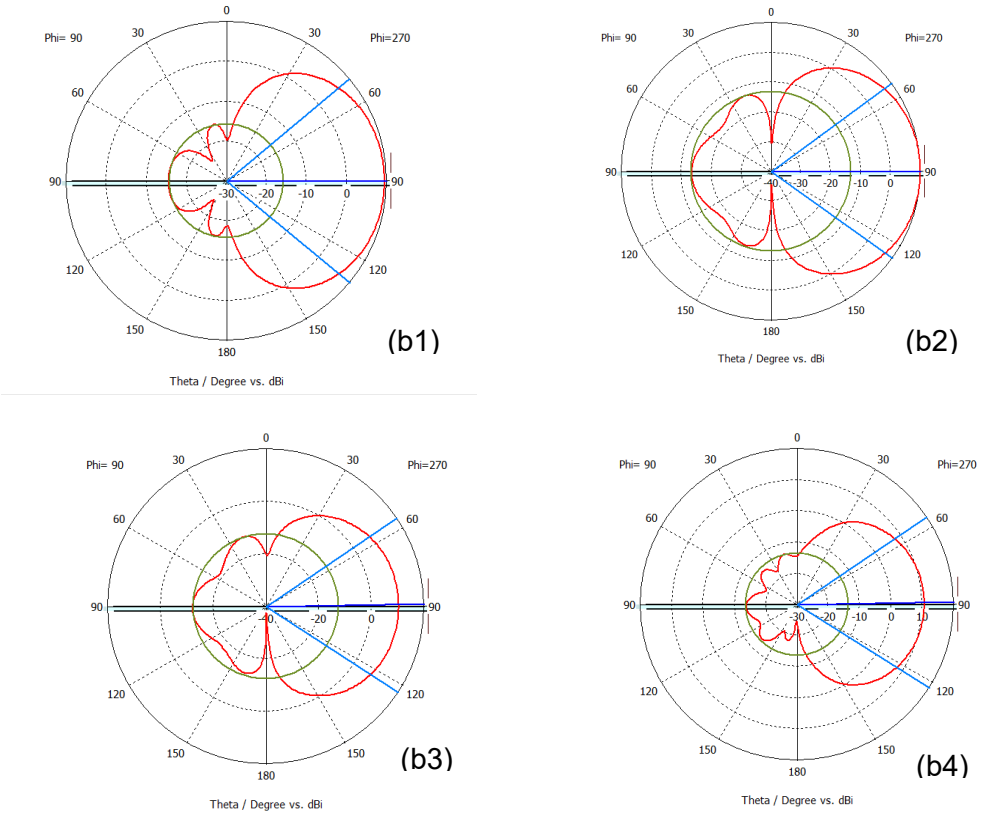


**Figure 11 1D far field polar plot of VPA antenna (b1) 2 GHz (b2) 2.5 GHz (b3) 3 GHz (b4) 4 GHz**



*This project is supported by funding from the Australian Government Department of Agriculture, Fisheries and Forestry as part of its Rural R&D for Profit programme in partnership with Research & Development Corporations, Commercial Companies, State Departments & Universities.*

The interaction of electromagnetic fields with biological tissue is dependent on dielectric properties($\varepsilon^* = \varepsilon' - j\sigma$, $\varepsilon'$ =permittivity and $\sigma$ = conductivity),and there exists a high contrast between skin, fat, muscle and bone .Based on these differing dielectric properties, electromagnetic waves are transmitted, absorbed, and reflected by each particular biological tissues in different ratios. In CST™ a simulation environment was created, with fat and muscle tissue layers containing dielectric values corresponding to sheep and cattle. Each antenna was tested in this simulation environment to determine how the electromagnetic waves interaction on tissue layers at different frequencies.

### 3.2.1 VPA antenna:

The VPA antenna electromagnetic waves interactions at 2 GHz and 2.5 GHz is shown in Fig. 12. The red colour is the radiation from the antenna source. In Fig. 12(a) the yellow and green coloured contours through the fat and muscle demonstrates that the electromagnetic waves are penetrating these tissues. However, in Fig. 12(b) the contours have reached the muscle layer however have not penetrated as deeply. As the frequency increased in Fig 12 (b) the electromagnetic fields also increased, thus the red coloured radiation is greater, and the gain of the antenna is higher.

Fig 13 shows the electromagnetic waves interactions at 3 GHz and 3.5 GHz. The penetration through the muscle in Fig. 13 (a) and (b) is decreased. However, the field of radiation and reflection has increased as demonstrated by the red colour, though the penetrations are not going into the muscle, as the frequency is beyond the tissue penetration range. Thus Fig 12 and Fig 13 demonstrate that for the VPA, as the frequency increases, the penetration of the electromagnetic waves into the tissues decreases significantly.



*This project is supported by funding from the Australian Government Department of Agriculture, Fisheries and Forestry as part of its Rural R&D for Profit programme in partnership with Research & Development Corporations, Commercial Companies, State Departments & Universities.*

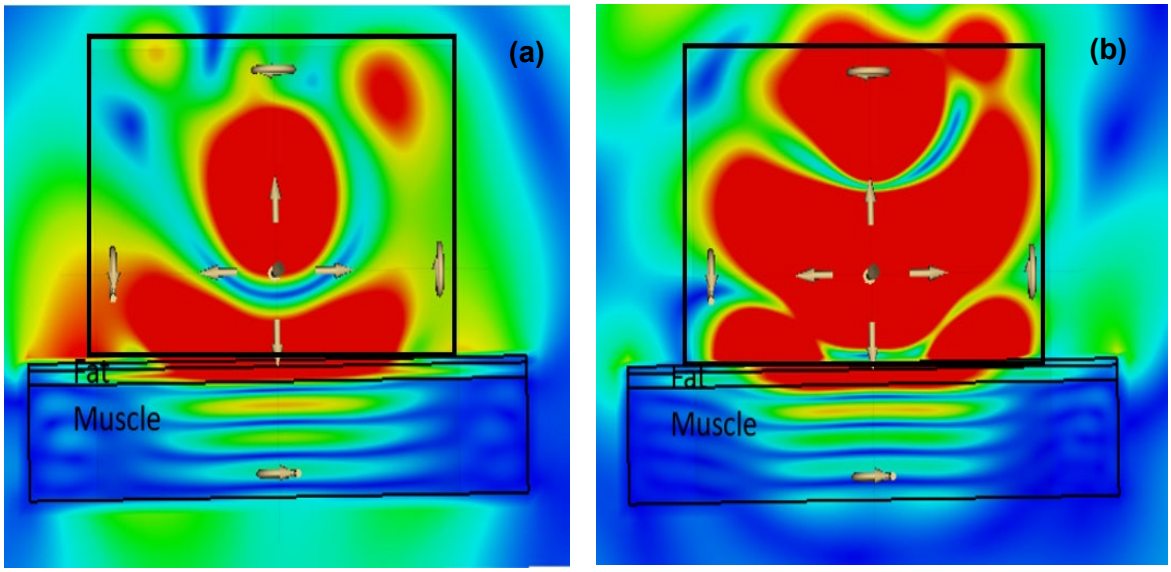


**Figure 12 VPA electromagnetic waves interaction on Tissues (a) At 2 GHz (b) 2.5 GHz**

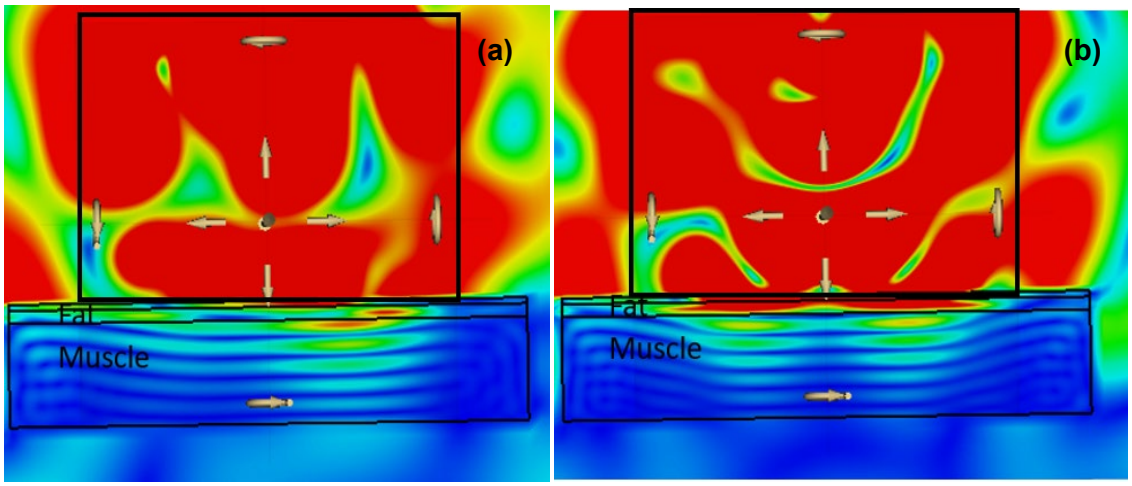


**Figure 13 VPA electromagnetic waves interaction on Tissues (a) At 3 GHz (b) 3.5 GHz**



*This project is supported by funding from the Australian Government Department of Agriculture, Fisheries and Forestry as part of its Rural R&D for Profit programme in partnership with Research & Development Corporations, Commercial Companies, State Departments & Universities.*

### 3.2.2 Open-ended coaxial probe

The OCP electromagnetic wave interactions at 2 GHz and 2.5 GHz is depicted in Fig 14. As demonstrated by the red colour, the radiation pattern of the OCP is directed down as it contacts the tissue surface. In Fig 14 (a) the yellow and green coloured contours penetrate completely through the fat and muscle layer however in Fig 14 (b) the contours don't quite reach the end of the muscle. Fig 14 shows the electromagnetic waves interactions at 3 GHz and 3.5 GHz. As the frequency increases, the yellow and green contours cannot penetrate as deeply into the muscle layers as depicted in Fig 15 (a) &(b).

In comparison to the VPA probe depicted in Fig 12. & Fig 13. the radiation pattern is confined to the tissue surface, making this a very suitable probe for near field measurements single site measurements.

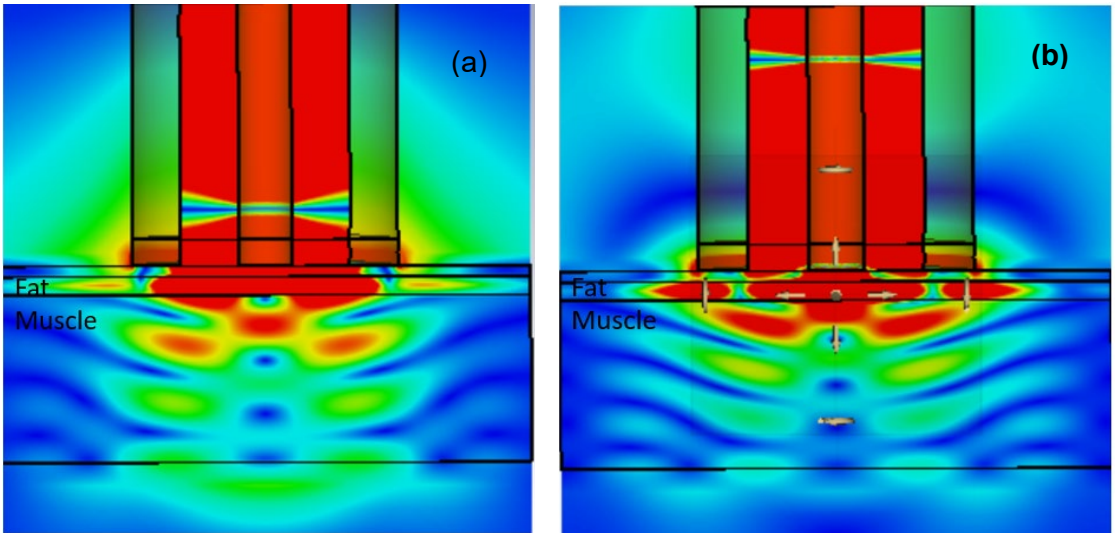


**Figure 14 OCP Electromagnetic waves interaction on Tissues (a) At 2 GHz (b) 2.5 GHz**

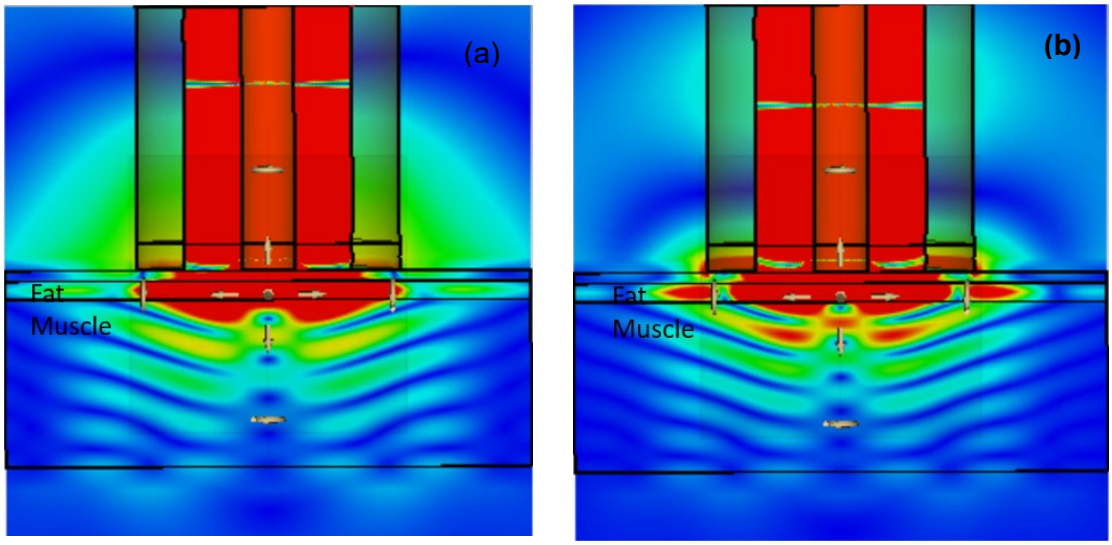


**Figure 15 OCP electromagnetic waves interaction on Tissues (a) At 3 GHz (b) 3.5 GHz**



*This project is supported by funding from the Australian Government Department of Agriculture, Fisheries and Forestry as part of its Rural R&D for Profit programme in partnership with Research & Development Corporations, Commercial Companies, State Departments & Universities.*

### 3.2.3 Periodic-log antenna

The PLA electromagnetic wave interactions at 2 GHz and 2.5 GHz is shown in Fig 16. In Fig 16(a) & (b) the electromagnetic waves are penetrating through the fat and muscle layers as demonstrated by the yellow and green contours. Typically, the gain of an antenna should increase as the frequency increases. However, in Fig 16(b), with an increased frequency, the red colour has decreased, demonstrating the gain has decreased. This indicates that the design of the PLA needs further optimisation to overcome this error.

Fig 17 (a) & (b) shows the electromagnetic waves interactions at an increased frequency of 3 GHz and 3.5 GHz. As the gain decreases here, the amount of red has also decreased, and the electromagnetic waves have barely penetrated into the muscle layer.

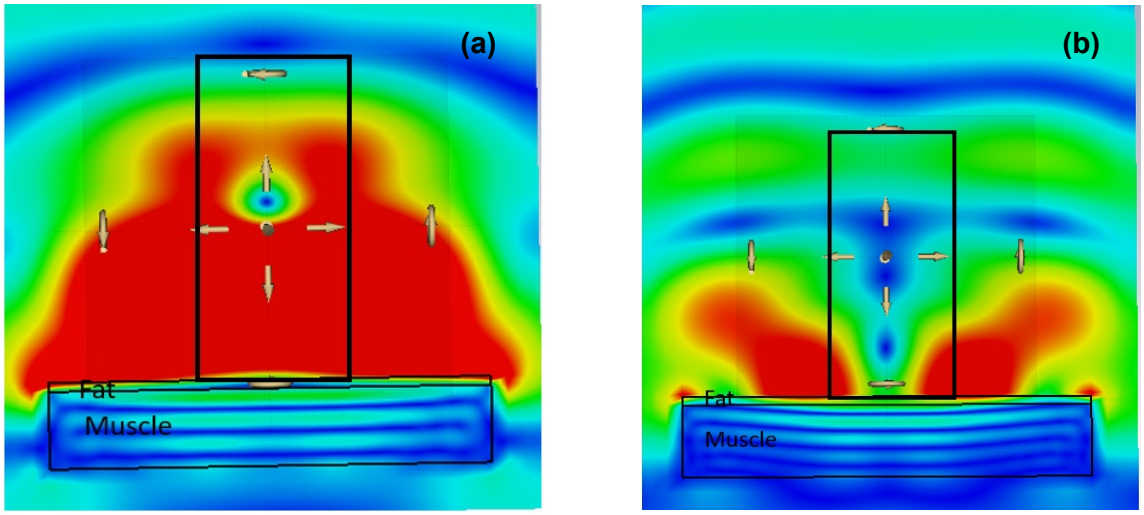


**Figure 16 PLA electromagnetic waves interaction on Tissues (a) At 2 GHz (b) 2.5 GHz**

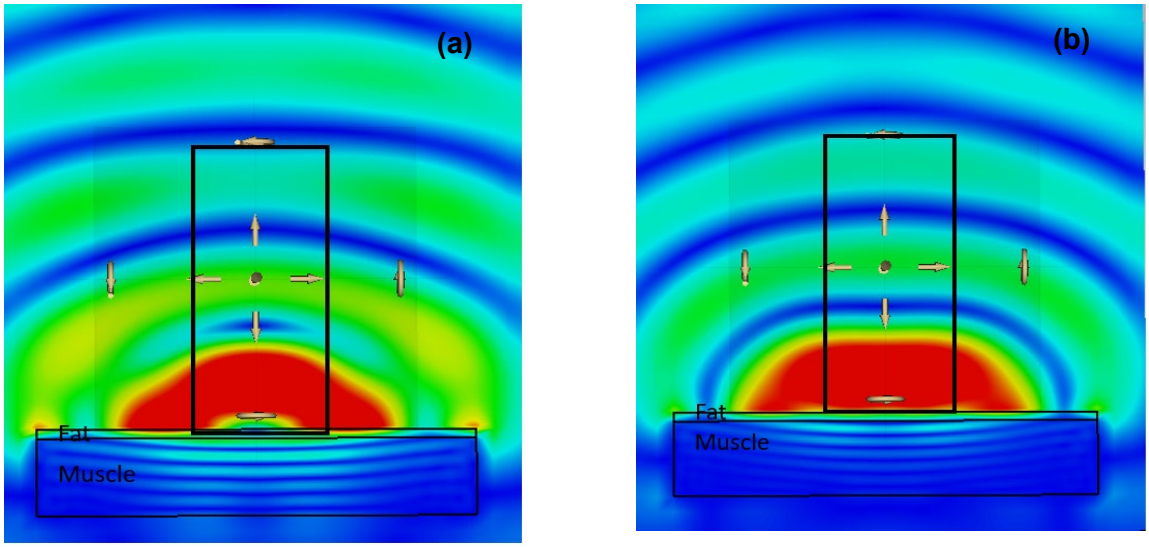


**Figure 17 PLA electromagnetic waves interaction on Tissues (a) At 2 GHz (b) 2.5 GHz**



*This project is supported by funding from the Australian Government Department of Agriculture, Fisheries and Forestry as part of its Rural R&D for Profit programme in partnership with Research & Development Corporations, Commercial Companies, State Departments & Universities.*

## 3.3 Discussion

The tissue simulations have demonstrated that the VPA has the widest radiation pattern. By covering a large tissue surface area, it is predicted that the VPA will allow for the testing of multiple traits (e.g. C-site and GR site) from one point microwave scanned on the carcase. The OCP radiation pattern was much smaller and confined to the probe surface region, which will be good for a single-site tissue depth measurements. The PLA antenna demonstrated a very high gain the low frequency of 2 GHz, which would be suitable for fat and muscle depth analysis, however at this frequency it won't allow for deep penetration which may not be suitable for traits such as eye muscle depth.

The electromagnetic wave interaction on tissue demonstrates that as the frequency increases, most of the waves are reflected and not penetrating into the tissues due to the high contrast between fat to muscle dielectric properties. To enable signal penetration deep into the tissues and ensure transfer of signals into the muscle, the new antennas should be compact in size, and designed to operate at a low frequency 0.7 GHz – 3GHz.

## 3.4 Conclusion

VPA, OCP and PLA in a simulation environment demonstrated good potential for measuring tissue depth at a low frequency.



*This project is supported by funding from the Australian Government Department of Agriculture, Fisheries and Forestry as part of its Rural R&D for Profit programme in partnership with Research & Development Corporations, Commercial Companies, State Departments & Universities.*

# 4 Experiment Two – commercial testing of antenna/probe

Three experiments were conducted to compare the precision and accuracy of VPA, OCP and PLA used to predict subcutaneous fatness in beef and lamb carcases.

## 4.1 Experiment A: Beef carcase PLA vs OCP

### 4.1.1 Experimental design

In this experiment one slaughter group of Hereford-Angus cross steers (n=147) were microwave scanned using a PLA and an OCP on the hot carcase at the P8 site approximately 45 minutes post-slaughter. The P8 site was manually recorded by accredited abattoir personnel using a cut knife ruler (Anonymous, 2005).

The methodology for microwave signal capture and analysis is detailed in full in Marimuthu *et al.* (2021a).

### 4.1.2 Statistical analysis

The prediction equations were constructed using a machine learning ensemble stacking method in WEKA® 3.9.4 (The University of Waikato, Hamilton, New Zealand) and detailed in Marimuthu et al., (2020; J. Marimuthu, K. M. Loudon, & G. Gardner, 2021b). In brief, the stacking method consisted of layering two prediction models to create a meta-algorithm (Elshazly, Elkorany, Hassanien, & Azar, 2013; Ribeiro & dos Santos Coelho, 2020). Layer one was composed from Support Vector Machine and Random Forest, and layer two used a Partial Least Squares Regression two component model.

The methodology for analysing the ability of VPA and PLA predict P8 fat depth was the same. The estimations were pooled based on antenna/probe (VPA/PLA) and randomly divided into 5 groups balanced for P8. A 5-fold cross validation was performed where the data was trained in 4 of the groups (80% of the data), and validated on the remaining 5$^{th}$ group (20%). This procedure was repeated such that every group was validated against, resulting in a total of 5 validation groups.

For all results, the precision of microwave scanning to predict the carcase measurement are expressed as root mean square error of the prediction (RMSEP) and R-square ($R^2$), with $R^2$ expressed within the text as the percentage (%) of the variation that the model describes. Bias and slope estimates represent the accuracy of the prediction model. The bias is the difference between the predicted and the actual values at the mean of the dataset, while the slope is the deviation of the slope of the relationship from 1. For average slope and bias calculations across the five validation groups, the absolute values |x| were used.



*This project is supported by funding from the Australian Government Department of Agriculture, Fisheries and Forestry as part of its Rural R&D for Profit programme in partnership with Research & Development Corporations, Commercial Companies, State Departments & Universities.*

### 4.1.3 Results

The PLA demonstrated the greatest precision of prediction of P8 fat depth with an average RMSEP of 1.29 mm, which was 0.28 mm less than the average OCP (*Table 1*). The average $R^2$ for PLA of 0.83 was 0.10 units higher than for the OCP (*Table 1*).

The average bias was slightly greater for the PLA at 0.350 mm compared to 0.249 mm for the OCP however across all validation groups the bias did not exceed more than 0.537 mm. There was minimal difference in average slope for the PLA compared to the OCP.

The association between actual and microwave predicted P8 fat depth for PLA and OCP are depicted in Fig. 18. The association between PLA and OCP are depicted in Fig. 19.

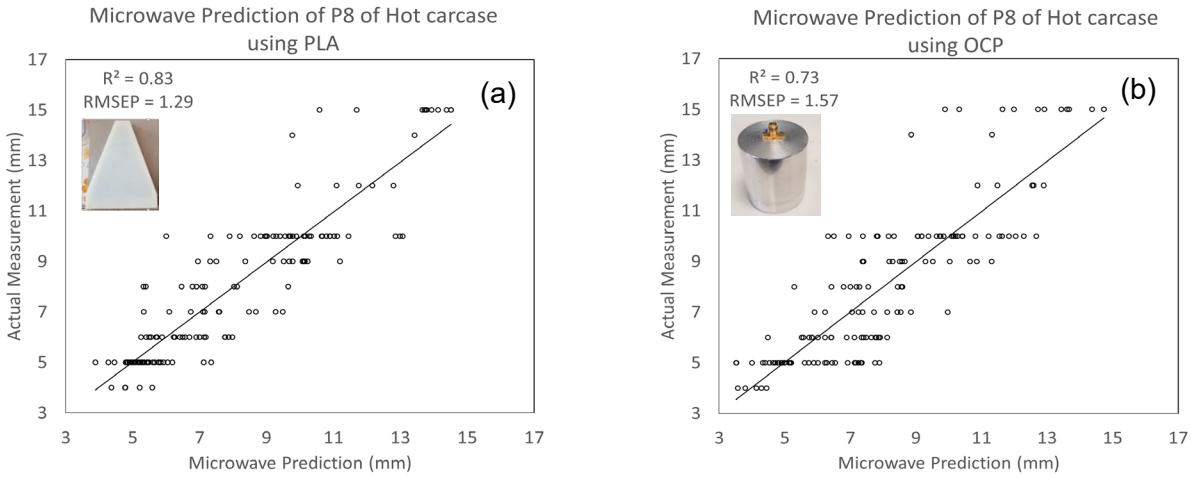


**Figure 18 The association between actual and microwave predicted P8 fat depth using the (a) PLA and (b) OCP. The predictions are derived from the validation tests detailed in Table 1. The actual tissue depths were regressed against the predictions. Solid lines represent the relationship between predicted and actual measurements.**

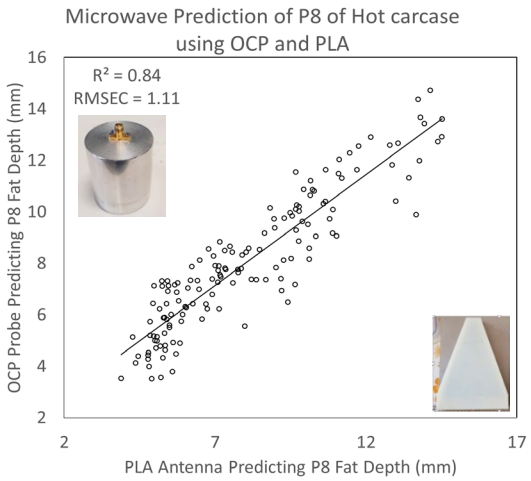


**Figure 19 The association between PLA and OCP. The predictions are derived from the validation tests detailed in Table 1. Solid line represents the relationship between the predicted measurements.**



*This project is supported by funding from the Australian Government Department of Agriculture, Fisheries and Forestry as part of its Rural R&D for Profit programme in partnership with Research & Development Corporations, Commercial Companies, State Departments & Universities.*

**Table 1 Precision and accuracy estimates for 5-fold cross validation of PLA and OCP to predict carcase P8 site fat depth. Precision estimates include R2 and root mean square error of the predicted (RMSEP). Accuracy estimates include slope which is the difference between the actual and predicted slopes, expressed as a deviation from 1, and bias which represents the difference between the actual minus predicted value calculated at the mean of the predicted site. Carcase P8 fat depth (mm) and Hot carcase weight (HCWT) (kg) values reported are mean ± standard deviation (minimum, maximum) of the raw values for each of the 5 validation groups.**

| | | | | Log Periodic Antenna (PLA) | | | | Open Ended Coaxial Probe (OCP) | | | |
|---|---|---|---|---|---|---|---|---|---|---|---|
| Validation Group | N in validation | HCWT (kg) | Carcase P8 (mm) | $R^2$ | RMSEP (mm) | Bias (mm) | Slope | $R^2$ | RMSEP (mm) | Bias (mm) | Slope |
| 1 | 29 | 319.77 ± 25.18 (278 – 363) | 8.17 ± 3.11 (5 – 15) | 0.88 | 1.13 | +0.352 | -0.02 | 0.82 | 1.34 | +0.226 | -0.13 |
| 2 | 29 | 307.44 ± 25.99 (258 – 353) | 8.10 ± 3.02 (5 – 15) | 0.75 | 1.55 | -0.252 | +0.13 | 0.60 | 1.90 | -0.069 | +0.12 |
| 3 | 29 | 303.62 ± 30.62 (246 – 365) | 8.14 ± 3.13 (4 – 15) | 0.86 | 1.17 | -0.099 | -0.02 | 0.69 | 1.71 | +0.017 | +0.04 |
| 4 | 30 | 299.10 ± 26.69 (230 – 361) | 7.93 ± 3.05 (4 – 15) | 0.86 | 1.25 | +0.537 | -0.13 | 0.77 | 1.47 | +0.537 | -0.08 |
| 5 | 30 | 302.87 ± 31.31 (247 – 365) | 7.90 ± 3.02 (4 – 15) | 0.82 | 1.35 | -0.509 | -0.04 | 0.78 | 1.45 | -0.397 | +0.03 |
| | Average | 306.49 ± 28.60* (230 – 365) | 8.05 ± 3.02* (4 – 15) | **0.83** | **1.29** | **0.350**** | **0.07**** | **0.73** | **1.57** | **0.249**** | **0.08**** |

*value represents the pooled mean ± SD of all animals. **mean of the absolute values.



*This project is supported by funding from the Australian Government Department of Agriculture, Fisheries and Forestry as part of its Rural R&D for Profit programme in partnership with Research & Development Corporations, Commercial Companies, State Departments & Universities.*

## 4.2 Experiment B: Lamb carcase VPA vs OCP

### 4.2.1 Experimental design

In this experiment three slaughter groups of lambs (n=180) were microwave scanned using a VPA and an OCP on the hot carcase at the C-site (45 mm from spine midline over the 12$^{th}$ rib) and GR-site (110 mm from spine midline over the 12$^{th}$ rib) approximately 1-2 hours post slaughter. The GR-site was manually recorded using the AUS-MEAT accredited GR-knife. The day following slaughter the carcases were split between the 12$^{th}$ and 13$^{th}$ rib and the C-site was measured using digital callipers (depth of subcutaneous fat (mm) over the loin eye muscle at the exposed cut surface, taken approximately 45 mm from the midline, corresponding to the deepest part of the longissimus muscle) (Anonymous, 2005).

The methodology for microwave signal capture and analysis is detailed in full in Marimuthu *et al.* (2021a).

### 4.2.2 Statistical analysis

The prediction equations were derived by the method described in Section 4.1.2.

The methodology for analysing the ability of the VPA to the OCP was the same. The estimations for each probe/antenna (VPA/OCP) across all slaughter groups were pooled according to tissue trait (C-site/GR site). The pooled estimations were divided into 5 groups balanced for tissue trait (C-site/GR site). A 5-fold cross validation procedure was performed as described in Section 4.1.2.

### 4.2.3 Results

The VPA demonstrated the greatest precision of prediction for both the C-site and the GR site (*Table 2*) compared to the OCP.

For C-site prediction (Table 2(a)) the average RMSEP of the VPA and OCP were similar, with only 0.10 mm difference, however the $R^2$ were markedly improved for the VPA prediction at 0.67 compared to 0.56 for OCP. The bias of the VPA was approximately 2.5 greater than the OCP bias however all bias across the 5 validation groups did not exceed 0.362 mm (Table 2(a)). The average slopes were similar for C-site prediction, 0.15 mm for the VPA compared to 0.12 mm for the OCP (Table 2(a)).

The associations between actual and microwave predicted C-site fat depth for VPA and OCP are depicted in Fig. 20. The association between VPA and OCP for C-site fat depth is depicted in Fig. 21.

For GR site prediction, the average RMSEP for the VPA was 0.51 mm less than for the OCP (Table 2(b)). Again, there was a 0.11 unit increase in the average $R^2$ value for the VPA probe (Table 2(b)). For GR prediction the accuracy indicators of bias and slope were also less for the VPA. The average bias for VPA was 0.08 mm lower than OCP, with no bias



*This project is supported by funding from the Australian Government Department of Agriculture, Fisheries and Forestry as part of its Rural R&D for Profit programme in partnership with Research & Development Corporations, Commercial Companies, State Departments & Universities.*

estimates exceeding 0.583 mm across the 5 validation groups (Table 2(b)). The average slope for VPA GR-site prediction was over half that of the OCP (Table 2(b)).

The associations between actual and microwave predicted GR tissue depth for VPA and OCP are depicted in Fig. 22. The association between VPA and OCP for GR tissue depth is depicted in Fig. 23.



*This project is supported by funding from the Australian Government Department of Agriculture, Fisheries and Forestry as part of its Rural R&D for Profit programme in partnership with Research & Development Corporations, Commercial Companies, State Departments & Universities.*

**Table 2 Precision and accuracy estimates for 5-fold cross validation of VPA and OCP to predict carcase (a) C-site fat depth and (b) GR-tissue depth. Precision estimates include R2 and root mean square error of the predicted (RMSEP). Accuracy estimates include slope which is the difference between the actual and predicted slopes, expressed as a deviation from 1, and bias which represents the difference between the actual minus predicted value calculated at the mean of the predicted site. Carcase C-site fat depth (mm), GR tissue depth (mm) and Hot carcase weight (HCWT) (kg) values reported are mean ± standard deviation (minimum, maximum) of the raw values for each of the 5 validation groups.**

| | | | | Vivaldi Patch Antenna (VPA) | | | | Open Ended Coaxial Probe (OCP) | | | |
|---|---|---|---|---|---|---|---|---|---|---|---|
| Validation Group | N in validation | HCWT (kg) | Carcase tissue depth (mm) | $R^2$ | RMSEP (mm) | Bias (mm) | Slope | $R^2$ | RMSEP (mm) | Bias (mm) | Slope |
| (a) C-site | | | | | | | | | | | |
| 1 | **36** | 24.31 ± 2.82 (20.3 – 32.0) | 3.49 ± 1.66 (0.99 – 7.50) | 0.74 | 0.87 | +0.088 | -0.21 | 0.58 | 1.08 | +0.083 | +0.10 |
| 2 | **36** | 24.07 ± 4.72 (14.9 – 36.2) | 3.24 ± 1.63 (0.86 – 7.42) | 0.72 | 0.92 | -0.362 | -0.02 | 0.68 | 0.96 | -0.032 | -0.30 |
| 3 | **36** | 24.66 ± 3.97 (19.0 – 34.9) | 3.47 ± 1.46 (0.99 – 8.20) | 0.64 | 0.90 | +0.053 | +0.18 | 0.54 | 0.98 | +0.028 | +0.11 |
| 4 | **36** | 24.23 ± 3.32 (19.5 – 30.5) | 3.35 ± 1.56 (0.43 – 6.57) | 0.51 | 1.08 | -0.062 | +0.09 | 0.43 | 1.16 | -0.090 | -0.02 |
| 5 | **36** | 24.25 ± 3.85 (18.5 – 34.2) | 3.31 ± 1.64 (0.91 – 9.44) | 0.72 | 0.91 | +0.195 | -0.24 | 0.59 | 1.03 | +0.059 | -0.09 |
| | Average | **24.31 ± 3.75*** **(14.9 – 36.2)** | **3.37 ± 1.57*** **(0.43 – 9.44)** | **0.67** | **0.94** | **0.152**** | **0.15**** | **0.56** | **1.04** | **0.058**** | **0.12**** |
| (b) GR site | | | | | | | | | | | |
| 1 | **36** | 24.96 ± 3.81 (19.2 – 32.7) | (16.14 ± 5.11) (6.50 – 29.00) | 0.76 | 2.59 | +0.016 | -0.21 | 0.67 | 3.01 | +0.232 | -0.22 |
| 2 | **36** | 24.37 ± 3.53 (19.8 – 35.2) | (15.26 ± 5.17) (5.50 – 26.00) | 0.81 | 2.24 | -0.164 | -0.06 | 0.74 | 2.81 | -0.265 | -0.33 |
| 3 | **36** | 24.60 ± 3.99 (19.0 – 36.2) | (16.07 ± 4.68) (7.00 – 31.00) | 0.51 | 3.28 | -0.103 | +0.15 | 0.49 | 3.48 | +0.120 | +0.26 |
| 4 | **36** | 24.01 ± 4.40 (14.9 – 34.9) | (15.81 ± 4.77) (4.50 – 25.00) | 0.59 | 3.04 | -0.468 | +0.03 | 0.37 | 3.85 | -0.583 | +0.20 |
| 5 | **36** | 23.43 ± 2.87 (20.1 – 32.7) | (15.67 ± 4.96) (6.00 – 33.00) | 0.67 | 2.83 | +0.445 | +0.01 | 0.53 | 3.39 | +0.415 | +0.03 |
| | Average | **24.31 ± 3.75*** **(14.9 – 36.2)** | **15.79 ± 4.89*** **(4.50 – 33.0)** | **0.67** | **2.80** | **0.239**** | **0.09**** | **0.56** | **3.31** | **0.323**** | **0.21**** |

*value represents the pooled mean ± SD of all animals. **mean of the absolute values.



*This project is supported by funding from the Australian Government Department of Agriculture, Fisheries and Forestry as part of its Rural R&D for Profit programme in partnership with Research & Development Corporations, Commercial Companies, State Departments & Universities.*

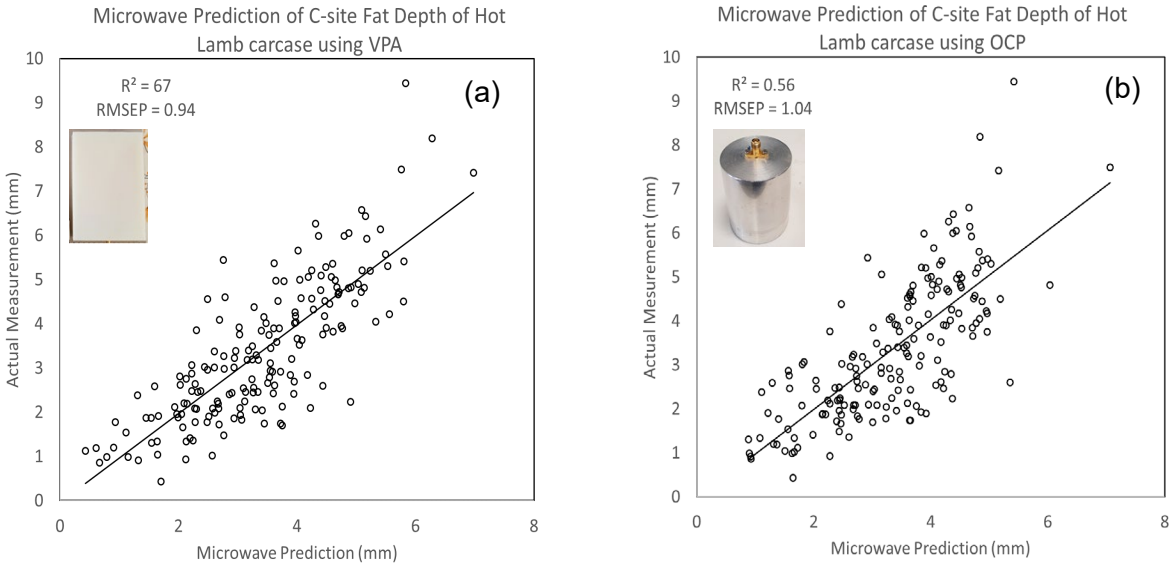


**Figure 20 The association between actual and microwave predicted C-site fat depth using the (a) VPA and (b) OCP. The predictions are derived from the validation tests detailed in Table 2(a). The actual tissue depths were regressed against the predictions. Solid lines represent the relationship between predicted and actual measurements.**

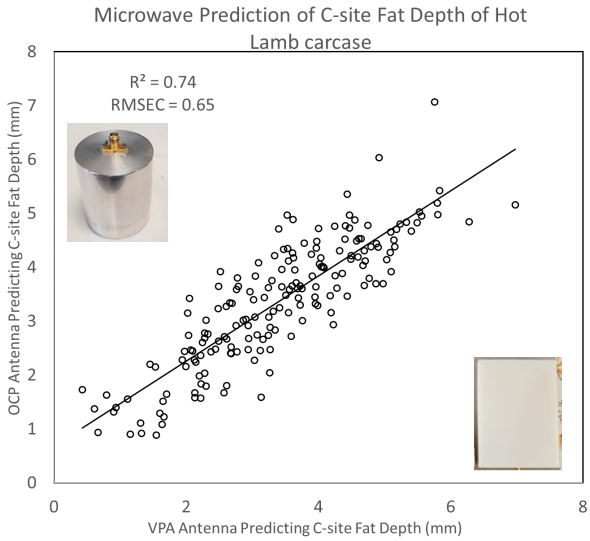


**Figure 21 The association between VPA and OCP for C-site fat depth prediction. The predictions are derived from the validation tests detailed in Table 2(a). Solid line represents the relationship between the predicted measurements.**



*This project is supported by funding from the Australian Government Department of Agriculture, Fisheries and Forestry as part of its Rural R&D for Profit programme in partnership with Research & Development Corporations, Commercial Companies, State Departments & Universities.*

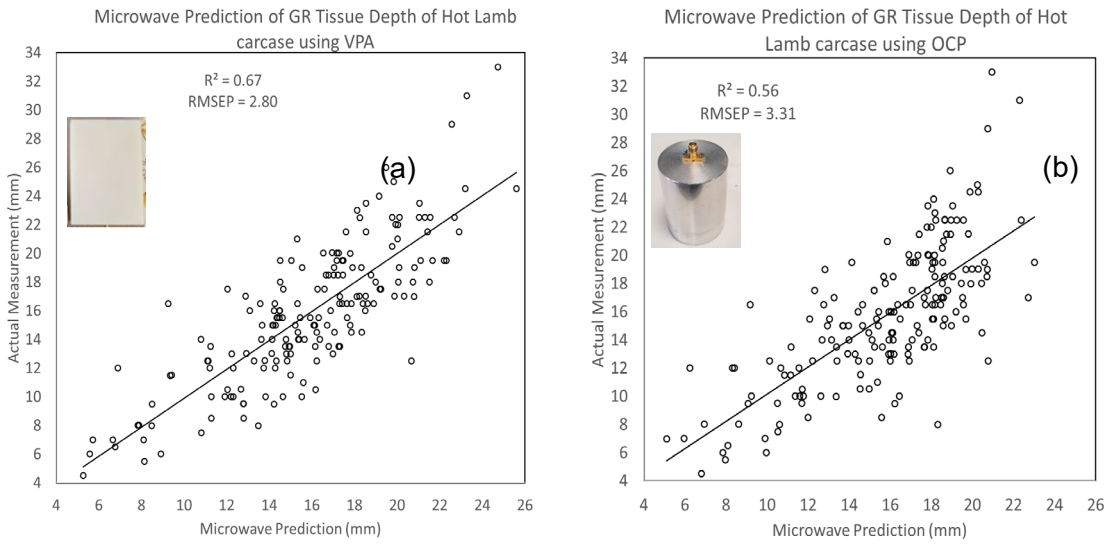


**Figure 22 The association between actual and microwave predicted GR tissue depth using the (a) VPA and (b) OCP. The predictions are derived from the validation tests detailed in Table 2(b). The actual tissue depths were regressed against the predictions. Solid lines represent the relationship between predicted and actual measurements.**

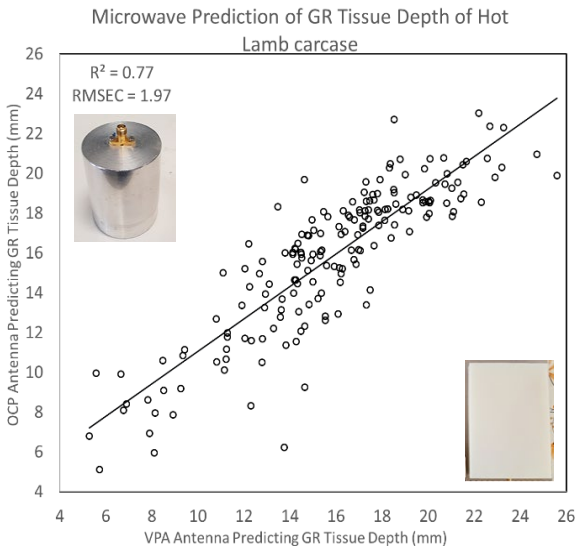


**Figure 23 The association between VPA and OCP for GR tissue depth prediction. The predictions are derived from the validation tests detailed in Table 2(b). Solid line represents the relationship between the predicted measurements.**



*This project is supported by funding from the Australian Government Department of Agriculture, Fisheries and Forestry as part of its Rural R&D for Profit programme in partnership with Research & Development Corporations, Commercial Companies, State Departments & Universities.*

## 4.3 Experiment C: Lamb carcase VPA vs PLA

### 4.3.1 Experimental design

In this experiment two slaughter groups of lambs (n=215) were microwave scanned using a VPA and an PLA on the hot carcase at the C-site and GR site within 1-2 hours post slaughter. C-site and GR site manual measurements were taken as described in Section 4.2.1.

The methodology for microwave signal capture and analysis is detailed in full in Marimuthu *et al.* (2021a).

### 4.3.2 Statistical analysis

The prediction equations were derived by the method described in Section 4.1.2.

For the predictions of VPA and PLA to determine C-site and GR tissue depth, a 5-fold cross validation was performed as described in Section 4.2.1.

### 4.3.3 Results

In the prediction of C-site fat depth, there was minimal difference in precision and accuracy indicators for the VPA compared to PLA (Table 3(a)). The average RMSEP differed by only 0.02 mm and the average $R^2$ differed by only 0.01 unit. The average bias was almost one third less for the PLA and the average slope was almost half for the PLA compared to the OCP.

For GR tissue depth prediction, the VPA had improved precision of prediction compared to the OCP (Table 3(b)). The average RMSEP for the VPA at 3.57 mm, was 13 mm lower than OCP. The average $R^2$ for VPA of 0.55 was 0.05 units higher than OCP. The average bias was highest for the VPA at 0.5 mm and across all validation groups the bias was almost 1 mm (Table 3(b)). The average slope for VPA at 0.18 mm was double that of the PLA antenna however all slopes had a deviation of less than 1/3 mm from 1.

The associations between actual and microwave predicted GR tissue depth for VPA and PLA are depicted in Fig. 24. The association between VPA and PLA for GR tissue depth is depicted in Fig. 25.



*This project is supported by funding from the Australian Government Department of Agriculture, Fisheries and Forestry as part of its Rural R&D for Profit programme in partnership with Research & Development Corporations, Commercial Companies, State Departments & Universities.*

**Table 3 Precision and accuracy estimates for 5-fold cross validation of VPA and PLA to predict carcase (a) C-site fat depth and (b) GR-tissue depth. Precision estimates include R2 and root mean square error of the predicted (RMSEP). Accuracy estimates include slope which is the difference between the actual and predicted slopes, expressed as a deviation from 1, and bias which represents the difference between the actual minus predicted value calculated at the mean of the predicted site. Carcase C-site fat depth (mm), GR tissue depth (mm) and Hot carcase weight (HCWT) (kg) values reported are mean ± standard deviation (minimum, maximum) of the raw values for each of the 5 validation groups.**

| | | | | Vivaldi Patch Antenna (VPA) | | | | Periodic log antenna (PLA) | | | |
|---|---|---|---|---|---|---|---|---|---|---|---|
| Validation Group | N in validation | HCWT (kg) | Carcase tissue depth (mm) | $R^2$ | RMSEP (mm) | Bias (mm) | Slope | $R^2$ | RMSEP (mm) | Bias (mm) | Slope |
| (a) C-site | | | | | | | | | | | |
| 1 | 43 | 27.49 ± 3.67 (20.5 – 34.2) | 3.94 ± 1.69 (1.38 – 9.44) | 0.65 | 0.99 | +0.033 | +0.06 | 0.67 | 0.96 | -0.032 | +0.03 |
| 2 | 43 | 27.22 ± 3.72 (19.4 – 34.4) | 3.81 ± 1.90 (0.63 – 9.08) | 0.72 | 1.00 | -0.123 | -0.04 | 0.66 | 1.10 | -0.027 | +0.02 |
| 3 | 43 | 27.72 ± 3.37 (20.3 – 35.4) | 3.88 ± 2.05 (1.39 – 9.66) | 0.68 | 1.19 | +0.210 | -0.18 | 0.73 | 1.10 | +0.006 | -0.21 |
| 4 | 43 | 27.58 ± 4.59 (18.3 – 35.6) | 3.48 ± 1.50 (0.73 – 8.33) | 0.67 | 0.87 | -0.138 | +0.10 | 0.69 | 0.83 | +0.054 | -0.00 |
| 5 | 43 | 26.38 ± 4.70 (17.6 – 36.2) | 3.69 ± 1.62 (0.97 – 7.42) | 0.58 | 1.05 | +0.008 | +0.12 | 0.59 | 1.03 | -0.048 | +0.05 |
| | Average | **27.28 ± 4.04* (17.6 – 36.2)** | **3.76 ± 1.75* (0.63 – 9.66)** | **0.66** | **1.02** | **0.102**** | **0.10**** | **0.67** | **1.00** | **0.033**** | **0.06**** |
| (b) GR site | | | | | | | | | | | |
| 1 | 43 | 27.74 ± 3.67) (18.5 – 34.9) | 18.73 ± 4.94 (8.50 – 31.00) | 0.58 | 3.17 | -0.025 | -0.07 | 0.52 | 3.38 | +0.142 | -0.01 |
| 2 | 43 | 26.55 ± 4.33) (18.3 – 36.2) | 18.30 ± 5.94 (5.00 – 31.00) | 0.58 | 3.94 | +0.513 | -0.20 | 0.45 | 4.39 | +0.135 | -0.02 |
| 3 | 43 | 27.61 ± 4.02) (18.6 – 33.7) | 18.47 ± 5.73 (10.00 – 33.00) | 0.54 | 3.94 | +0.909 | -0.08 | 0.54 | 3.92 | +0.614 | -0.13 |
| 4 | 43 | 27.49 ± 3.97) (19.0 – 35.4) | 17.56 ± 4.50 (8.00 – 30.00) | 0.40 | 3.66 | -0.150 | +0.27 | 0.43 | 3.47 | -0.404 | +0.10 |
| 5 | 43 | 27.03 ± 4.27) (17.6 – 35.6) | 17.87 ± 4.97 (8.00 – 29.00) | 0.64 | 3.13 | -0.905 | -0.26 | 0.55 | 3.35 | -0.284 | -0.21 |
| | Average | **27.28 ± 4.04* (17.6 – 36.2)** | **18.09 ± 5.03 (5.0 – 33.0)** | **0.55** | **3.57** | **0.500**** | **0.18**** | **0.50** | **3.70** | **0.316**** | **0.09**** |

*value represents the pooled mean ± SD of all animals. **mean of the absolute values.



*This project is supported by funding from the Australian Government Department of Agriculture, Fisheries and Forestry as part of its Rural R&D for Profit programme in partnership with Research & Development Corporations, Commercial Companies, State Departments & Universities.*

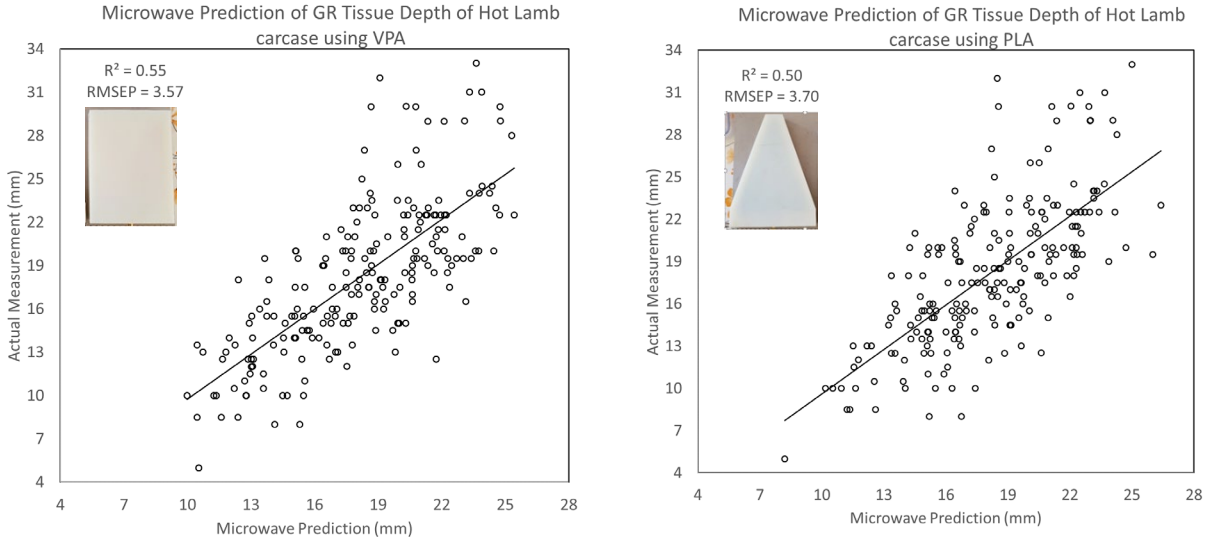


**Figure 24 The association between actual and microwave predicted GR tissue depth using the (a) VPA and (b) PLA. The predictions are derived from the validation tests detailed in Table 3(b). The actual tissue depths were regressed against the predictions. Solid lines represent the relationship between predicted and actual measurements.**

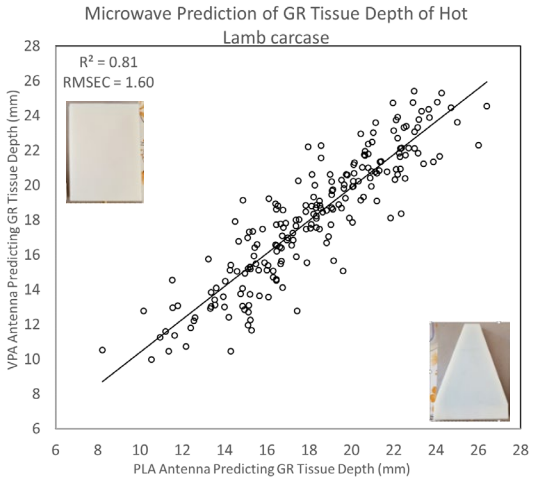


**Figure 25 The association between VPA and PLA for GR tissue depth prediction. The predictions are derived from the validation tests detailed in Table 2(b). Solid line represents the relationship between the predicted measurements.**



*This project is supported by funding from the Australian Government Department of Agriculture, Fisheries and Forestry as part of its Rural R&D for Profit programme in partnership with Research & Development Corporations, Commercial Companies, State Departments & Universities.*

## 4.4 Discussion

For beef carcase single site subcutaneous fatness prediction, the PLA demonstrated far greater performance than the OCP. For lamb carcase prediction the VPA and PLA gave similar performance, which was again far greater than the OCP. The improved performance of the VPA and PLA is likely due to their wide radiation pattern giving a larger exposure on the tissue surface. The field of radiation pattern for the VPA and PLA is similar, as demonstrated in Fig. 4 and Fig. 11, equating to an arc approximately 120 mm x 80 mm from center of antenna contact on the carcase. The gain of the PLA is high at low frequencies with little backscattering as demonstrated in Fig 16(a), thus suitable for small tissue depth measurements such as subcutaneous fat.

The precision of the VPA to predict GR tissue depth was significantly less in Experiment C compared to Experiment B. It is unclear why there was such a large error in this measurement and further training and validation using the VPA across a wider range of slaughter days is required to determine any environmental affect impacting the precision of prediction.

While the OCP probe did not perform as well for single site fatness prediction in beef and lamb, with a smaller radiation pattern that has greater penetration, we predict that this probe may be more suited for deeper tissue depth measurements such as eye muscle depth and intramuscular fat % prediction.

## 4.5 Conclusion

Overall, the results demonstrate that the VPA and PLA can predict single site subcutaneous fatness in beef and lamb. Further validation and training is required at chain speed, across multiple devices and multiple operators is required.



*This project is supported by funding from the Australian Government Department of Agriculture, Fisheries and Forestry as part of its Rural R&D for Profit programme in partnership with Research & Development Corporations, Commercial Companies, State Departments & Universities.*

# 5 References


Anonymous. (2005). *Handbook of Australian Meat* (7th ed.). Brisbane Australia: AUS-MEAT Limited.

Elshazly, H. I., Elkorany, A. M., Hassanien, A. E., & Azar, A. T. (2013). Ensemble classifiers for biomedical data: performance evaluation. *2013 8th International Conference on Computer Engineering & Systems (ICCES)*, 184-189. doi: 10.1109/ICCES.2013.6707198

Marimuthu, J., Loudon, K., & Gardner, G. (2021a). Report on the validation of a prototype microwave device to measure fat depth at the rib and P8 sites on live cattle and validate against the corresponding ultrasound and abattoir measurements.

Marimuthu, J., Loudon, K. M., & Gardner, G. (2020). Prediction of lamb carcase C-site fat depth and GR tissue depth using a non-invasive portable microwave system. *Meat Science*, 108398.

Marimuthu, J., Loudon, K. M., & Gardner, G. (2021b). Ultrawide band microwave system as a non-invasive technology to predict beef carcase fat depth. *Meat Science*, 108455. doi: 10.1016/j.meatsci.2021.108455

Pozar, D. M. (2011). *Microwave engineering*: John wiley & sons.

Ribeiro, M. H. D. M., & dos Santos Coelho, L. (2020). Ensemble approach based on bagging, boosting and stacking for short-term prediction in agribusiness time series. *Applied Soft Computing, 86*, 105837. doi: 10.1016/j.asoc.2019.105837

Sushko, O., Piltyay, S., & Dubrovka, F. (2020, 21-25 Sept. 2020). *Symmetrically Fed 1–10 GHz Log-Periodic Dipole Antenna Array Feed for Reflector Antennas.* Paper presented at the 2020 IEEE Ukrainian Microwave Week (UkrMW).




*This project is supported by funding from the Australian Government Department of Agriculture, Fisheries and Forestry as part of its Rural R&D for Profit programme in partnership with Research & Development Corporations, Commercial Companies, State Departments & Universities.*